

Y3.N21/5:6/2077

NACA TN 2077

# NATIONAL ADVISORY COMMITTEE FOR AERONAUTICS

## TECHNICAL NOTE 2077

A DETERMINATION OF THE LAMINAR-, TRANSITIONAL-, AND  
TURBULENT-BOUNDARY-LAYER TEMPERATURE-RECOVERY  
FACTORS ON A FLAT PLATE IN SUPERSONIC FLOW

By Jackson R. Stalder, Morris W. Rubesin,  
and Thorval Tendeland

Ames Aeronautical Laboratory  
Moffett Field, Calif.



Washington

June 1950

CONN. STATE LIBRARY

JUN 12 1950

BUSINESS, SCIENCE  
& TECHNOLOGY DEPT.





NATIONAL ADVISORY COMMITTEE FOR AERONAUTICS

TECHNICAL NOTE 2077

A DETERMINATION OF THE LAMINAR-, TRANSITIONAL-, AND  
TURBULENT-BOUNDARY-LAYER TEMPERATURE-RECOVERY  
FACTORS ON A FLAT PLATE IN SUPERSONIC FLOW

By Jackson R. Stalder, Morris W. Rubesin,  
and Thorval Tendeland

SUMMARY

Wind-tunnel tests have been performed to determine the temperature-recovery factors for laminar, transitional, and turbulent boundary layers on a flat plate. The tests were performed at a nominal Mach number of 2.4 and data were obtained over a Reynolds number range from  $0.235 \times 10^6$  to  $6.75 \times 10^6$ .

Identification of the type of boundary layer present on the test body was made by an evaluation of the velocity distribution within the boundary layer. These data were obtained through use of a small impact pressure tube.

It was found that the temperature-recovery factor for a laminar boundary layer on a flat plate had the value 0.881. The corresponding value for a fully developed turbulent boundary layer resulting from natural transition varied from 0.897 to 0.884 along the plate. The maximum possible error in measurement of these values of recovery factor is estimated as  $\pm 0.007$ .

NOTATION

- M Mach number, dimensionless
- n exponent of exponential velocity distribution, dimensionless
- Pr Prandtl number, dimensionless
- r temperature-recovery factor, dimensionless
- Re Reynolds number, dimensionless



T	absolute temperature, °F absolute
U	velocity, feet per second
x	distance from leading edge of plate, feet
y	distance normal to plate, feet
$\gamma$	ratio of specific heats, dimensionless
$\delta$	boundary-layer thickness, feet
$\theta$	momentum thickness, feet (defined by equation (10))
$\mu$	absolute viscosity, pound-seconds per square foot
$\nu$	kinematic viscosity, feet squared per second
$\rho$	slugs per cubic foot

#### Subscripts

aw	adiabatic wall
1	local free-stream conditions
o	stagnation conditions

#### INTRODUCTION

Knowledge of the temperature recovery at the surfaces of insulated bodies in high-speed compressible flow is prerequisite to investigations of convective heat transfer under similar conditions. Existing information concerning the temperature recovery in compressible boundary layers at supersonic speeds is relatively meager. A summary of the results of several analytic investigations of the temperature recovery for the case of a laminar boundary layer on a flat plate is given in reference 1. The summary indicates that the temperature-recovery factor  $r$  defined by the equation

$$T_{aw} = T_1 \left( 1 + r \frac{\gamma-1}{2} M_1^2 \right) \quad (1)$$

is independent of the Mach and Reynolds numbers and depends solely upon the Prandtl number. The consensus of these analytical results is that



$$r = Pr^{1/2} \quad (2)$$

when  $0.72 < Pr < 1.2$ ,  $0 < M < 10$ , and the temperature exponent for viscosity and thermal conductivity varies from 0.5 to 1.25. The question as to whether the Prandtl number is to be evaluated at the free-stream temperature, the adiabatic surface temperature, or some intermediate temperature is left unanswered by all the solutions since each imposed the condition that the Prandtl number was invariant within the boundary layer. Although there is some uncertainty as to the values of Prandtl number for air over the range of temperatures encountered in wind tunnels, there are indications that it varies from 0.705 to 0.750 over the range of temperatures from  $100^{\circ}$  F to  $-200^{\circ}$  F. (See references 2 through 5.)

The preceding analytical results were substantiated somewhat by Eber (reference 6) who performed tests on insulated cones. It is possible to compare recovery-factor data of cones with that of flat plates by eliminating the effect of the cone angle through the use of the free-stream velocity and temperature behind the attached conical shock wave. Eber found  $r = 0.85 \pm 0.025$  for a Mach number range from 1.2 to 3.1.

Recently a more thorough investigation of the recovery factors on bodies of revolution at supersonic speeds was made by Wimbrow (reference 7). It was found that at  $M = 2$  the laminar recovery factor on a cone is approximately 0.858. It was determined also that the recovery factor is not affected appreciably by the pressure distribution on a parabolic body of revolution at  $M = 2.0$ , varying only from 0.855 to 0.861 along the length of the body. Variations from 0.848 to 0.860 for different tests with the same parabolic body were attributed to a slight variation of surface roughness.

No analytical investigations exist for Prandtl numbers other than unity in which the variation of fluid properties in the turbulent boundary layer is considered. For Prandtl numbers other than unity and for the case of constant fluid properties, Ackermann (reference 8) has determined values of the recovery factor which can be well represented by

$$r = Pr^{1/3} \quad (3)$$

in the region  $0.5 < Pr < 2$ .

Other analyses, summarized in reference 9, which account for frictional dissipation in a constant-property turbulent boundary layer are:

1. The analysis by Seban which results in

$$r = 1 - (4.71 - 4.11B - 0.601 Pr) Re^{-0.2} \quad (4)$$

where



$$B = \frac{\text{Pr} (5\text{Pr} - 7)}{2 (5\text{Pr} + 1)}$$

2. The work of Shirokow which gives

$$r = 1 - 4.55 (1 - \text{Pr}) \text{Re}^{-0.2} \quad (5)$$

Each of these solutions is based on a boundary-layer-velocity distribution determined experimentally by Nikuradse; however, the latter solution is further restricted in that it neglects the buffer layer. (The buffer layer is defined as that region in the turbulent boundary layer which lies between the completely turbulent and the completely laminar regions.)

3. The analysis of Squire results in the approximate expression

$$r = \text{Pr}^{\frac{n+1}{n+3}} \quad (6)$$

where  $n$  is the exponent of the exponential velocity distribution used. As  $n$  is known to change slightly with Reynolds number, it is noted that each of the last three solutions indicates some variation of recovery factor with the Reynolds number. The imposed condition of incompressibility in each case, however, eliminates Mach number as a variable.

A few experiments have been performed to determine recovery factors in turbulent boundary layers at supersonic speeds. The early work of Kraus on a cylinder with its axis parallel to the flow (reference 6) indicates a recovery-factor variation with Mach number. The values determined were 0.979 at  $M = 4.38$  and 0.910 at  $M = 1.86$ . However, there is some question as to the existence of steady-state conditions during these experiments. E. Eckert (reference 9) found the recovery factor on a flat plate to range in value from 0.915 to 0.898 at a nominal Mach number equal to 1.75.

The tests described previously for the laminar boundary layer were repeated by Wimbrow (reference 7) with artificially induced turbulent boundary layers. It was found that the value of the recovery factor on the cone was 0.888 at  $M = 2.0$ . On the parabolic body of revolution the values of the recovery factor were 0.891 and 0.902 at  $M = 2.0$  and 1.5, respectively. It is interesting to note that the recovery factors were constant along the length of the parabolic body, even though a variable pressure existed.

The data indicated above are summarized in the following table:



Type of boundary layer	Author	Model	Mach number	Recovery factor
Laminar	Eber	Cone	1.2 to 3.1	0.85 ± 0.25
	Wimbrow	Cone	2	.858
	Wimbrow	Parabolic body of revolution	2	.855 - .861
	Wimbrow	Parabolic body of revolution (slight variation of surface roughness)	2.0 to 2.2	.848 - .860
Turbulent	Kraus	Cylinder, axis parallel to flow	4.38	.979
	Eckert	Flat plate	1.86	.910
	Wimbrow	Cone <sup>1</sup>	1.75	.915 - .898
	Wimbrow	Cone <sup>1</sup>	2.00	.888
	Wimbrow	Parabolic body <sup>1</sup> of revolution	2.00	.891
			1.50	.902

<sup>1</sup>Artificially induced transition.

It is apparent from the preceding summary that no data exist for the laminar boundary layer on a flat plate. Although the laminar boundary layers on bodies of revolution can be related mathematically to those on flat plates, the physical phenomena resulting from leading-edge shock waves, oscillations in the boundary layer, free-stream turbulence, etc., are not considered in the mathematics and may act differently in the two cases. Data in the transitional region of bodies are also nonexistent, while the data in the turbulent boundary layer resulting from natural transition are rather uncertain. In view of this, it was the purpose of the present investigation to determine the local temperature-recovery factors in each of the three boundary-layer regimes on a flat-plate model. Identification of the type of boundary layer was achieved by measuring the local velocity distribution through the boundary layer with a small impact pressure probe.

The relationship between the stagnation temperature and static temperature for an adiabatic process is

$$T_0 = T_1 \left( 1 + \frac{\gamma-1}{2} M_1^2 \right) \quad (7)$$

Because the air flow in the wind tunnel is essentially adiabatic when temperature equilibrium is achieved, the stagnation temperature is constant throughout the tunnel. The stagnation temperature is a measurable quantity and it may be determined as a static-temperature measurement in a region of low air velocity. As the static temperature  $T_1$  is not measurable, it is eliminated from equations (1) and (7) and there is obtained



$$r = 1 - \frac{T_o - T_{aw}}{T_o} \left[ \frac{2}{(\gamma-1) M_1^2} + 1 \right] \quad (8)$$

From equation (8), it is seen that the quantities required for determining the local recovery factor are: the stagnation temperature  $T_o$ , the adiabatic surface temperature  $T_{aw}$ , and the local Mach number  $M_1$ .

#### DESCRIPTION OF EQUIPMENT

##### The Ames 6-Inch Heat-Transfer Wind Tunnel

The Ames 6-inch heat-transfer tunnel is a return-type continuously operating tunnel which is designed to obtain heat-transfer data at supersonic speeds. The tunnel is equipped with removable nozzle blocks, and, by changing nozzle blocks, it is possible to obtain a range of Mach numbers of from 1.8 to 2.8. Only one set of nozzle blocks, designed for a nominal Mach number of 2.4, was used for these tests. The actual test-section size for these particular nozzle blocks is approximately 5-1/2 by 5-1/2 inches.

A sketch of the major components of the wind tunnel is shown in figure 1. The air in the tunnel is circulated by means of a four-stage centrifugal compressor driven by a three-phase induction motor with a rating of 1500 horsepower at 2600 rpm. By varying the frequency of the current to the motor, any speed throughout the speed range of the compressor may be obtained. The compressor is driven by the motor through speed-increasing gears.

The air temperature in the tunnel is controlled by means of an air cooler located in the large circular section of the tunnel upstream from the test section. Cooling water which is circulated through the air cooler is obtained from a forced-draft cooling tower located outside the tunnel building. Temperature control is effected by means of an automatic controller which throttles the water flow through the air cooler. This controller maintains the stagnation temperature to within  $\pm 0.5^\circ$  F of any desired temperature between  $75^\circ$  F and  $150^\circ$  F. An air mixer is located downstream from the air cooler to improve the temperature distribution of the air before entering the test section. The air mixer consists of five baffles which deflect the air flow back and forth across the tunnel. The turbulence of the air after passing through the mixer is then reduced by means of a series of six wire screens spaced at 6-inch intervals. The screens are 14 mesh with a wire diameter of 0.02 inch.

The stagnation temperature of the air in the tunnel is measured by means of 20 calibrated iron-constantan thermocouples. These thermocouples are spaced along horizontal and vertical diameters in the large circular portion of the tunnel at the entrance to the test section. Radiation



losses from the thermocouples are minimized by surrounding each thermocouple with a radiation shield. Conduction and radiation heat losses from the tunnel itself are reduced by lagging, which consists of approximately 1-1/2 inches of rock wool. This lagging also provides sound insulation.

Supply air for the tunnel is furnished by means of a reciprocating air compressor. Before entering the tunnel, the supply air is passed through a silica-gel air dryer where the moisture content is reduced to a specific humidity of approximately 0.0001 pound of water per pound of dry air. The tunnel stagnation pressure is controlled between 2 and 54 pounds per square inch absolute by means of an automatic pressure controller which maintains any desired pressure between these levels to within  $\pm 0.05$  pound per square inch. Operation at stagnation pressures above atmospheric is effected by bleeding dry air into the tunnel from a high-pressure storage tank. Subatmospheric stagnation pressures are maintained by means of a vacuum pump which evacuates the tunnel to the desired pressure.

Atmospheric air is prevented from leaking into the tunnel at the compressor shaft by means of carbon-ring seals. In this arrangement, a pressure differential is maintained across the seal by means of a vacuum pump so that any air leakage through the seal is outward from the compressor to the atmosphere. Flow visualization in the test section is achieved by use of a conventional two-mirror schlieren system utilizing 12-inch-diameter circular mirrors of 180-inch focal length.

#### Description of Model

The flat-plate model used for the tests, shown schematically in figure 2, was constructed from stainless steel. The model was 16 inches long, approximately 5-1/2 inches wide, and 1/2 inch thick. The upstream end was chamfered to form an angle of  $15^\circ$ , and the leading edge was rounded to a radius of about 0.003 inch to avoid feathering. The region from 2.2 inches to 8.7 inches from the leading edge was the testing region. A 3/8-inch-deep by 3-inch-wide groove was milled in the bottom of the plate along the center line to permit the installation of thermocouples. Similar grooves 1/2 inch wide were milled in the bottom of the plate along the sides to permit the installation of pressure orifices. A 1/16-inch-thick cover plate on the bottom sealed these grooves and formed a dead-air space providing insulation between the top and bottom of the plate. The thermocouples were made of calibrated iron and constantan wires peened 1/4 inch apart, spanwise, to the inside of the top surface of the plate. As the thermocouple junction was formed through the stainless steel, these thermocouples measured the temperature 1/16 inch below the top surface. They were placed on 1/2-inch centers along the center line of the plate. The static-pressure orifices were 0.0135 inch in diameter and were located in a line 1 inch from each side of the plate. The chordwise distance between orifices on each side of the plate was 2 inches; however, these



orifices were staggered 1 inch with respect to those on the other side of the plate, thereby allowing pressure readings at 1-inch intervals along the plate. The top surface of the plate was ground and polished to a mirror-like finish.

The support for the flat-plate model consisted of a steel plate, 3/4 inch thick, which was bolted to the rear portion of the test plate. The supporting plate was secured to removable side plates in the tunnel walls downstream from the testing region. Both the test plate and the supporting plate spanned the test section and could be rotated to change the plate angle of attack if desired. Additional support to prevent the test plate from bending and vibrating was achieved by doweling the plate to the tunnel walls and by fastening thin strips of soft fabric to the sides of the test plate. The strips of fabric provided bearing surfaces between the glass windows on either side of the test section.

#### TEST PROCEDURE

The test conditions were chosen so as to provide a range of Reynolds numbers of from  $0.235 \times 10^6$  to  $6.75 \times 10^6$  based on the length along the plate. This range of Reynolds numbers was obtained by varying the stagnation pressure of the wind tunnel from 5 to 45 psia at intervals of 5 psia. The stagnation temperature was maintained at a nominal value of  $100^\circ$  F for all the tests.

The Mach number variation along the plate was obtained from the readings of the static-pressure orifices located in the plate surface and the reading of an impact-pressure probe placed 0.250 inch from the plate surface and 7 inches from the leading edge of the plate. The impact-pressure probe was about 2 inches forward of the position where the shock wave, originating at the leading edge of the plate and reflected from the top nozzle block, struck the boundary layer of the plate. From the readings of the impact-pressure probe and the static-pressure orifice, at the same axial distance along the plate, it was possible to determine the true stagnation pressure within the shock triangle over the plate. This stagnation pressure, in conjunction with the static-pressure readings, allowed the determination of the Mach number distribution along the plate. The impact pressures were measured with a mercury manometer, and the static pressures were measured with dibutyl-phthalate manometers. All these manometers were referred to a high vacuum, the absolute magnitude of which was determined by a McLeod gage.

The temperature distributions along the axis of the plate were measured simultaneously with the afore-mentioned pressure measurements. A recording potentiometer was used to indicate the voltage of the 20 stagnation-temperature thermocouples and of the 14 plate-surface thermocouples. When steady state was indicated by this instrument, a manual-balancing potentiometer was connected to the thermocouple circuit and accurate voltage readings were made.



When the recovery-factor tests were completed, impact-pressure surveys were made in the boundary layer of the plate to identify the type of boundary layer which produced the measured recovery factors. The probe used in these boundary-layer surveys was constructed of flattened hypodermic tubing. The opening of the probe was approximately 0.013 inch high and 0.080 inch wide. The time lag to obtain a pressure measurement with the probe connected to a mercury manometer was of the order of 2 minutes. The height of the boundary-layer probe above the surface of the plate was measured with a dial indicator located on the vertical post of a cathetometer. The least count of this dial indicator was 0.0001 inch. The telescope of the cathetometer was sighted through a test-section window on a fine line scribed on the probe. This line was parallel to the surface of the plate and sufficiently high above the lower edge of the probe to be outside the boundary layer and thereby eliminate refraction effects. It is estimated that the position of the probe could be measured to about  $\pm 0.001$  inch.

In some tests, artificial transition from a laminar to a turbulent boundary layer was induced by two methods. The first device used to promote transition was a 0.012-inch-diameter wire cemented to the plate surface parallel to and  $3/8$  inch downstream from the leading edge of the plate. The second device used to promote transition was a  $1/2$ -inch-wide band of lamp black cemented to the leading edge of the plate.

#### DISCUSSION OF RESULTS

The maximum possible error in the measurement of the recovery-factor data of this report is estimated to be approximately  $\pm 0.7$  percent. The basis for this estimate is as follows: The stagnation temperature in the tunnel was known to  $\pm 0.5^\circ$  F because all the stagnation-temperature-thermocouple readings were within  $\pm 0.5^\circ$  F of the average stagnation temperature, and the thermocouple wire was calibrated to  $\pm 0.25^\circ$  F. The manual-balancing potentiometer used to read the voltage of these thermocouples could be read within these limits. The plate thermocouples could measure temperatures to within  $\pm 0.1^\circ$  F as determined from the thermocouple calibration and the readings of the manual-balancing potentiometer. However, evaluation of the effects of radiation and of the maximum axial heat conduction along the plate and through the air gap within the plate indicate that a maximum error of  $\pm 1.4^\circ$  F is possible. An estimate of the accuracy of the Mach number determination, based on the least readings of the manometers used, indicates that the Mach number is known to  $\pm 0.01$ . There is, however, a maximum variation of Mach number across the wind tunnel equal to 0.05 as indicated by the static-pressure orifices. A static-pressure survey along the center line of the plate has indicated pressures which are between those given by the static orifices on the sides of the plate. Therefore, it is estimated that the Mach number along the center line is half way between the extremes given by the plate static-pressure orifices and is known to  $\pm 0.025$ . The possible error of the local



recovery factor resulting from these individual errors can be determined by the definition of the total differential of the recovery factor:

$$|dr| \leq \left| \frac{\partial r}{\partial T_o} dT_o \right| + \left| \frac{\partial r}{\partial T_{aw}} dT_{aw} \right| + \left| \frac{\partial r}{\partial M_1} dM_1 \right| \quad (9)$$

To obtain the maximum possible error, the absolute values of each side of equation (9) are taken. When the above errors are introduced into this equation, and the values  $\partial r/\partial T_o$ ,  $\partial r/\partial T_{aw}$ , and  $\partial r/\partial M_1$  are determined from equation (8), it is found that the differential  $dr$  has a value of 0.7 percent.

The variation of the Mach number at the outer edge of the boundary layer of the flat plate for three of the pressure levels tested is shown in figure 3. These data are representative of all the data taken. It is found that the Mach number distribution is slightly different for each pressure level. The small variation in Mach number with pressure level is believed to be due to the variation in the effective area of the nozzle caused by the boundary layers on the wind-tunnel walls and on the model. As the pressure increases, the boundary-layer thickness decreases and the effective area ratio and Mach number increase.

In general, it may be noted that the Mach number is uniform over the first 4 inches of the plate. No data could be taken at the 5-inch position as the pressure tap there developed a leak. The maximum variation of the free-stream Mach number is about 3 percent. It should be noted that the value of 3 percent includes the effect of the reflected bow shock wave which strikes the plate at about 9 inches from the leading edge.

In figure 4 are shown several velocity distributions used for identifying the type of boundary layer which produces the particular temperature-recovery factor measured. These velocity distributions were computed from impact pressure and plate static-pressure readings using the assumption that the total temperature throughout the boundary layer was constant. This assumption is shown in reference 10 to give results which are within about 1.5 percent of those evaluated using the true static temperature. No attempt was made to ascertain the effective probe position error produced by the mutual interference of the impact pressure probe and the surface of the plate. The velocity distributions are shown in terms of the ratio of the distance normal to the plate surface to the momentum thickness. The momentum thickness is defined as

$$\theta = \int_0^{\delta} \frac{\rho U}{\rho_1 U_1} \left( 1 - \frac{U}{U_1} \right) dy \quad (10)$$

The integral in equation (10) is evaluated from the data by numerical integration.



In general, it is noted that the velocity distributions are of two types. The data taken at a stagnation pressure of 20 psia and a Reynolds number of  $1.37 \times 10^6$  and that taken at 5 psia at Reynolds numbers of  $0.64 \times 10^6$  and  $0.32 \times 10^6$  exhibit essentially identical characteristics. These velocity profiles compare well in shape, if not in magnitude, with the theoretical laminar velocity distribution obtained from the method of reference 11. The reasons for the discrepancy between the data and theory are not known; however, the experimental points are sufficiently close to the theoretical curve to identify the boundary layers as laminar. The data taken at a stagnation pressure of 40 psia and a Reynolds number of  $5.22 \times 10^6$  show that the boundary-layer velocity profiles in dimensionless form are essentially the same whether the boundary layer is tripped artificially or not. As the data compare in form with a representative theoretical curve determined from the analysis of Frankl and Voishel (reference 12), it is concluded that the boundary layer is turbulent. Although these turbulent-boundary-layer velocity distributions have essentially the same characteristics when the data points are plotted in dimensionless form, it should be noted that the tripped boundary layer is actually one and one-half times as thick as the one resulting from natural transition. This fact will be used in explaining some of the temperature-recovery-factor characteristics exhibited in the next figure. No attempt was made to obtain a transitional-boundary-layer velocity distribution.

The local temperature-recovery factors, plotted as a function of Reynolds number, are shown in figure 5. The characteristic dimension used in the Reynolds number is the distance from the leading edge of the plate, and the air properties used are evaluated at the free-stream temperature. The data for the various pressure levels are plotted together. Three sets of data with artificially tripped boundary layers are also included.

The data show the local recovery factor to be practically constant with Reynolds number in the laminar region, to rise slowly in the transition region, and to drop gradually in the fully turbulent region. Minute examination of the data, however, indicates that the boundary between the laminar and transitional regions in terms of Reynolds number depends on the pressure level. Although these variations are well within the estimated accuracy of the results, the phenomenon indicated by the consistency of the data is worth mentioning. The data obtained at a stagnation pressure of 5 psia exhibit a deviation from their constant laminar value of 0.881 at  $Re = 0.56 \times 10^6$ , while the data obtained at a stagnation pressure of 10 psia deviate from this same value of recovery factor at  $Re = 0.93 \times 10^6$ . Similar deviations are observed for the laminar-boundary-layer recovery factors which were attained at higher pressure levels.

In addition to this effect of pressure level on the beginning of transition, there is also an effect of pressure level on the value of the recovery factor of the laminar boundary layer. It can be observed that the laminar-boundary-layer recovery factors increase slightly with increasing tunnel pressure level, rising to a value of 0.887 at a stagnation



pressure of 25 psia. The causes of these combined effects, a slightly increasing laminar-boundary-layer recovery factor and a delayed inception of transition, are not known but may be due to factors which vary with pressure level such as tunnel turbulence level, etc.

The recovery factor for a laminar boundary layer,  $r = 0.881$ , is  $1-1/2$  percent and 4 percent higher than the theoretical value given by  $Pr^{1/2}$ , depending on whether the free-stream or the surface temperature is used in evaluating the air properties. The reason why the results obtained do not lie somewhere between the limiting theoretical values is not readily apparent. Perhaps some variable not taken into account in the analyses, but occurring in the physical case, such as surface roughness, may cause this effect. (See reference 7).

For Reynolds numbers greater than  $2 \times 10^6$ , the boundary layer is fully turbulent. The values of recovery factor obtained with a turbulent boundary layer with natural transition present vary from 0.897 to 0.884 in the range of Reynolds numbers of from  $2 \times 10^6$  to  $6.7 \times 10^6$ . The values of recovery factor obtained from the artificially tripped turbulent boundary layer are slightly lower than the values obtained from the turbulent boundary layer caused by natural transition. This can be explained by the fact that the turbulent boundary layers effectively start at different points. Thus, when the turbulent boundary layer resulting from artificial tripping is one and one-half times as thick as the one resulting from natural transition, the effective length Reynolds numbers of the two are not the same. It is known from the  $1/7$ -power-law velocity distribution, when applied to an incompressible fluid, that the length Reynolds numbers of two turbulent boundary layers vary as shown in the following equation:

$$\frac{Re_1}{Re_2} = \left( \frac{\delta_1}{\delta_2} \right)^{1.25} \quad (11)$$

If equation (11) is arbitrarily applied to the present data, it is found that the ratio of the Reynolds numbers of the artificially tripped boundary layer to those of the boundary layer occurring from natural transition is about 1.65. It can be seen that, if the Reynolds numbers of the tripped boundary-layer data were multiplied by 1.65, both sets of data would correlate extremely well.

Although the existing turbulent-boundary-layer theories are inapplicable to a compressible boundary layer, it is observed that the data are bracketed by the limiting values of recovery factor calculated from equation (6), using air properties evaluated at free-stream and surface temperatures in the computation of the Prandtl number. The value of  $n$  used in equation (6) was one-fifth and was determined from the data shown in figure 4. It can also be seen that the values of recovery factor computed from equation (6) fit the data more closely than the values computed from the expression,  $r = Pr^{1/3}$ .



## CONCLUSIONS

The following conclusions can be drawn from the results of the present tests:

1. For the case of a laminar boundary layer on a flat plate, the temperature-recovery factor was found to be 0.881. This value is 4 percent and 1.5 percent larger than the theoretical values given by the square root of the Prandtl number when the air properties are evaluated at the plate surface temperature and the tunnel free-stream temperature, respectively.

2. The temperature-recovery factor, for the case of a turbulent boundary layer resulting from natural transition, varied from 0.897 to 0.884 in the range of Reynolds number from  $2 \times 10^6$  to  $6.7 \times 10^6$ . These values lie between the theoretical values of 0.898 and 0.884 computed from Squire's equation for a  $1/5$ -power-law velocity distribution using air properties evaluated at the surface and at the free-stream temperature, respectively.

Ames Aeronautical Laboratory,  
National Advisory Committee for Aeronautics,  
Moffett Field, Calif., Jan. 30, 1950.

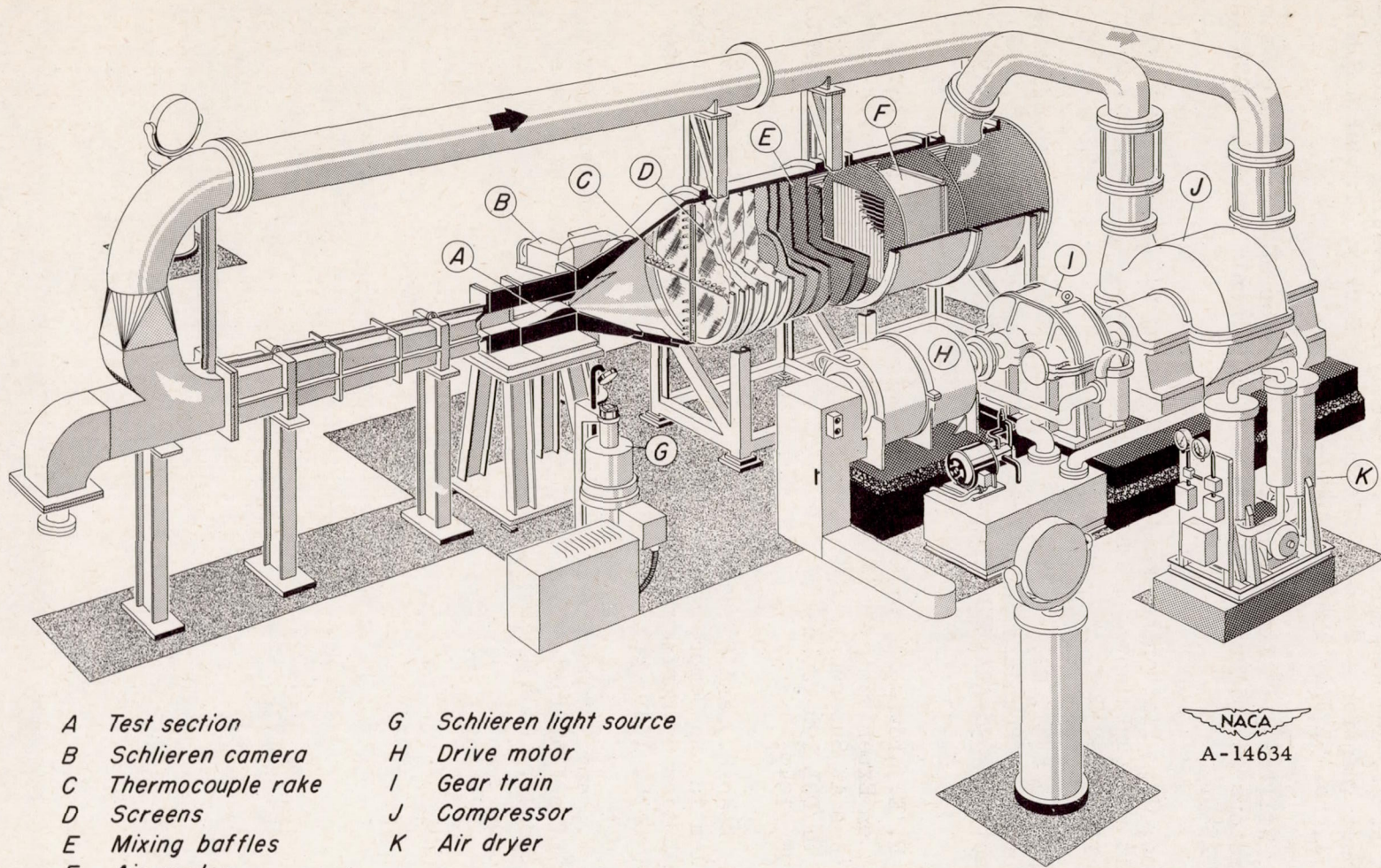
## REFERENCES

1. Rubesin, M. W., and Johnson, H. A.: A Critical Review of Skin-Friction and Heat-Transfer Solutions of the Laminar Boundary Layer of a Flat Plate. Trans. A.S.M.E., vol. 71, no. 4, May 1949, pp. 383-388.
2. Taylor, W. J., and Johnson, H. L.: An Improved Hot Wire Cell for Accurate Measurements of Thermal Conductivities of Gases over a Wide Temperature Range,  $87^\circ$  K -  $375^\circ$  K. Jour. of Chem. Physics, vol. 14, no. 4, Apr. 1946, pp. 219-233.
3. Johnston, Herrick L., and McCloskey, Kenneth E.: Viscosities of Several Common Gases between  $90^\circ$  K and Room Temperature. Jour. of Physical Chem., vol. 44, no. 9, Dec. 1940, pp. 1038-1058.
4. Tribus, Myron, and Boelter, L. M. K.: An Investigation of Aircraft Heaters. II - Properties of Gases. NACA ARR 132, Oct. 1942.
5. Cope, W. F., and Hartree, D. R.: The Laminar Boundary Layer in Compressible Flow. Trans. Phil. Roy. Soc. of London, series A, vol. 241, June 22, 1948, pp. 1-69.



6. Johnson, H. A., and Rubesin, M. W.: Aerodynamic Heating and Convective Heat Transfer - Summary of Literature Survey. Trans. A.S.M.E., vol. 71, no. 5, July 1949, pp. 447-456.
7. Wimbrow, William R.: Experimental Investigation of Temperature Recovery Factors on Bodies of Revolution at Supersonic Speeds. NACA TN 1975, 1949.
8. Ackermann, G.: Plattenthermometer in Stromung mit grosser Geschwindigkeit und turbulenter Grenzschicht. Ing.-Wes., vol. 13, no. 6, 1942, pp. 226-235.
9. Seban, R. A., Bond, R., and Varga, S. A.: Adiabatic Wall Temperature for Turbulent Boundary Layer Flow over Flat Plates. Rep. 6, AAF contract W33-038-AC-15229, Dept. of Engr., Univ. of Calif., Apr. 29, 1949.
10. Wilson, R. E., Young, E. C., and Thompson, M. J.: Second Interim Report on Experimentally Determined Turbulent Boundary Layer Characteristics at Supersonic Speeds. University of Texas, Defense Res. Lab., UT/DRL 196 (Johns Hopkins Univ., Applied Physics Lab., CM501), Jan. 25, 1949.
11. Chapman, Dean R., and Rubesin, Morris W.: Temperature and Velocity Profiles in the Compressible Laminar Boundary Layer with Arbitrary Distribution of Surface Temperature. Jour. Aero. Sci., vol. 16, no. 9, Sept. 1949, pp. 547-565.
12. Frankl, F., and Voishel, V.: Turbulent Friction in the Boundary Layer of a Flat Plate in a Two-Dimensional Compressible Flow at High Speeds. NACA TM 1053, 1943.





- |                            |                                 |
|----------------------------|---------------------------------|
| <i>A</i> Test section      | <i>G</i> Schlieren light source |
| <i>B</i> Schlieren camera  | <i>H</i> Drive motor            |
| <i>C</i> Thermocouple rake | <i>I</i> Gear train             |
| <i>D</i> Screens           | <i>J</i> Compressor             |
| <i>E</i> Mixing baffles    | <i>K</i> Air dryer              |
| <i>F</i> Air cooler        |                                 |

NACA  
A-14634

Figure 1.— Diagram of the Ames 6-inch heat-transfer wind tunnel.







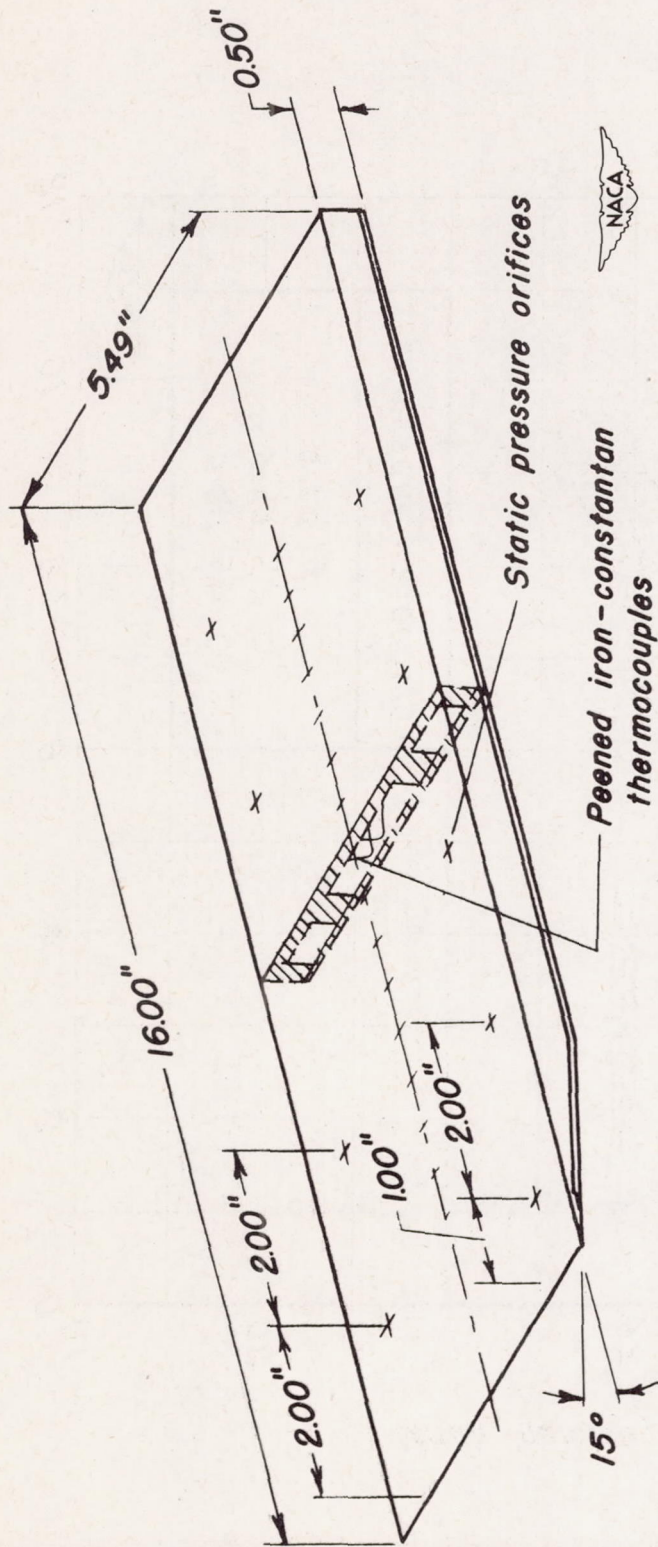


Figure 2.- Sketch of the flat-plate model.



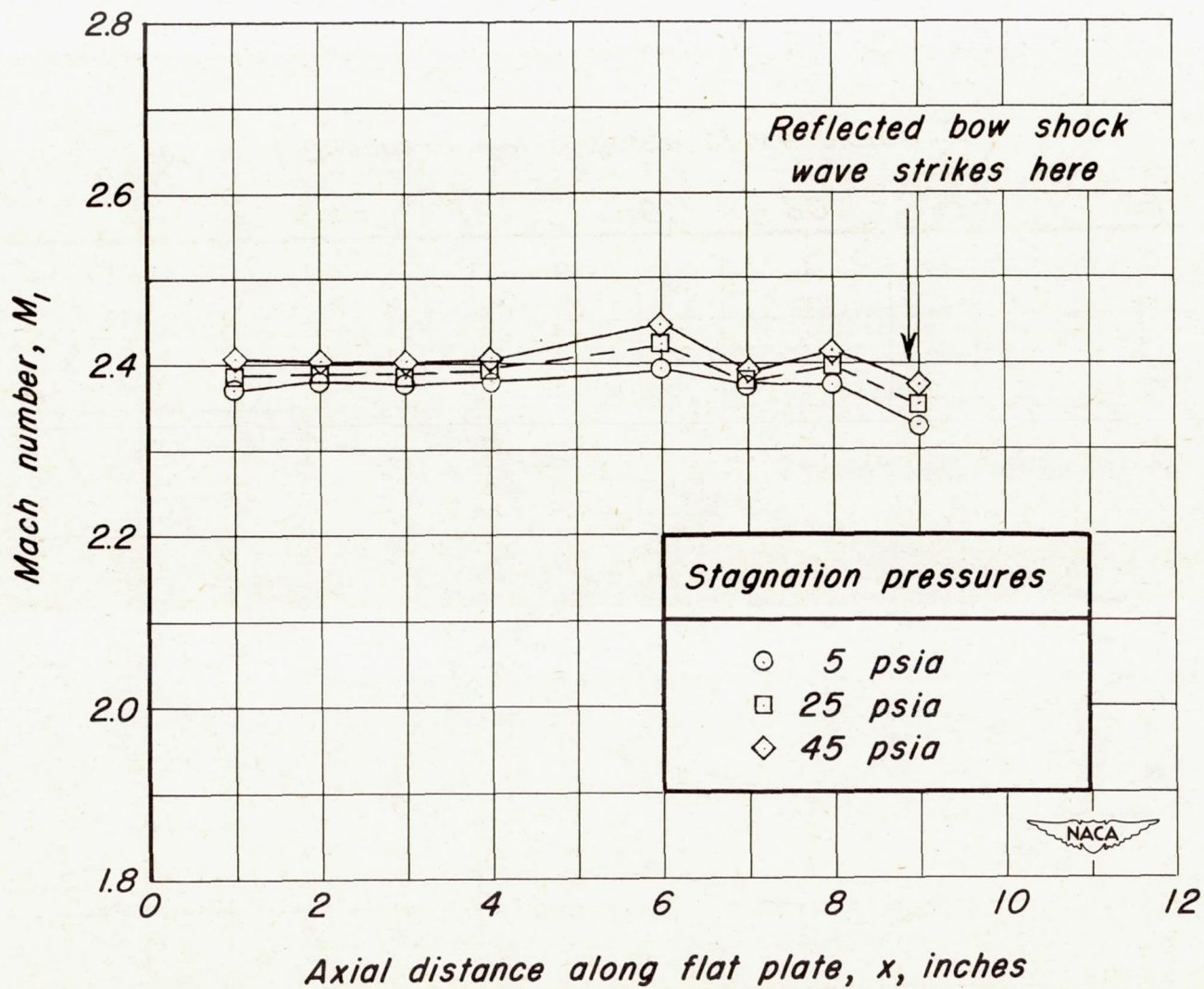


Figure 3.- Mach number distribution along axis of the flat plate.



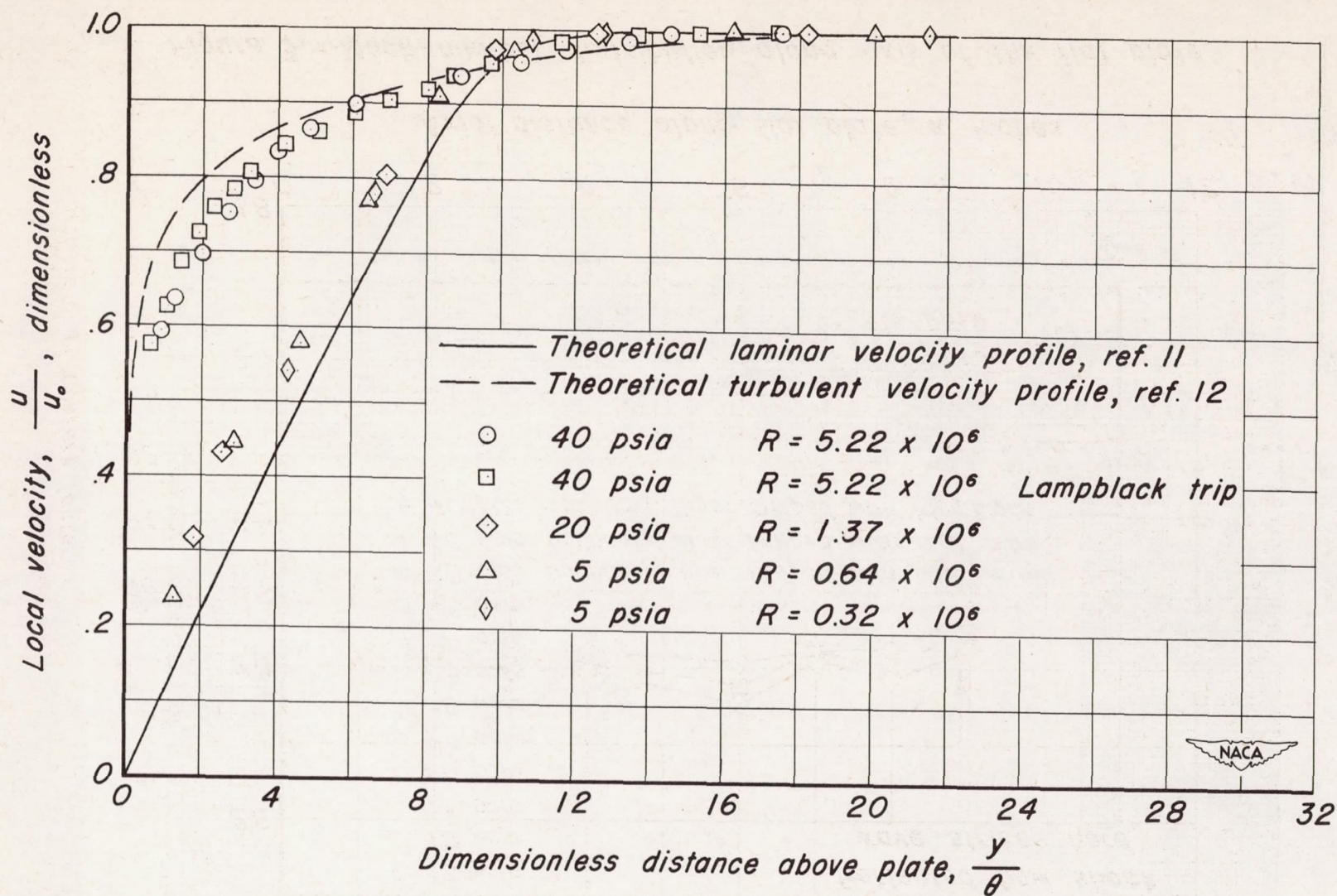


Figure 4.-Velocity distribution curves for identifying boundary-layer types.



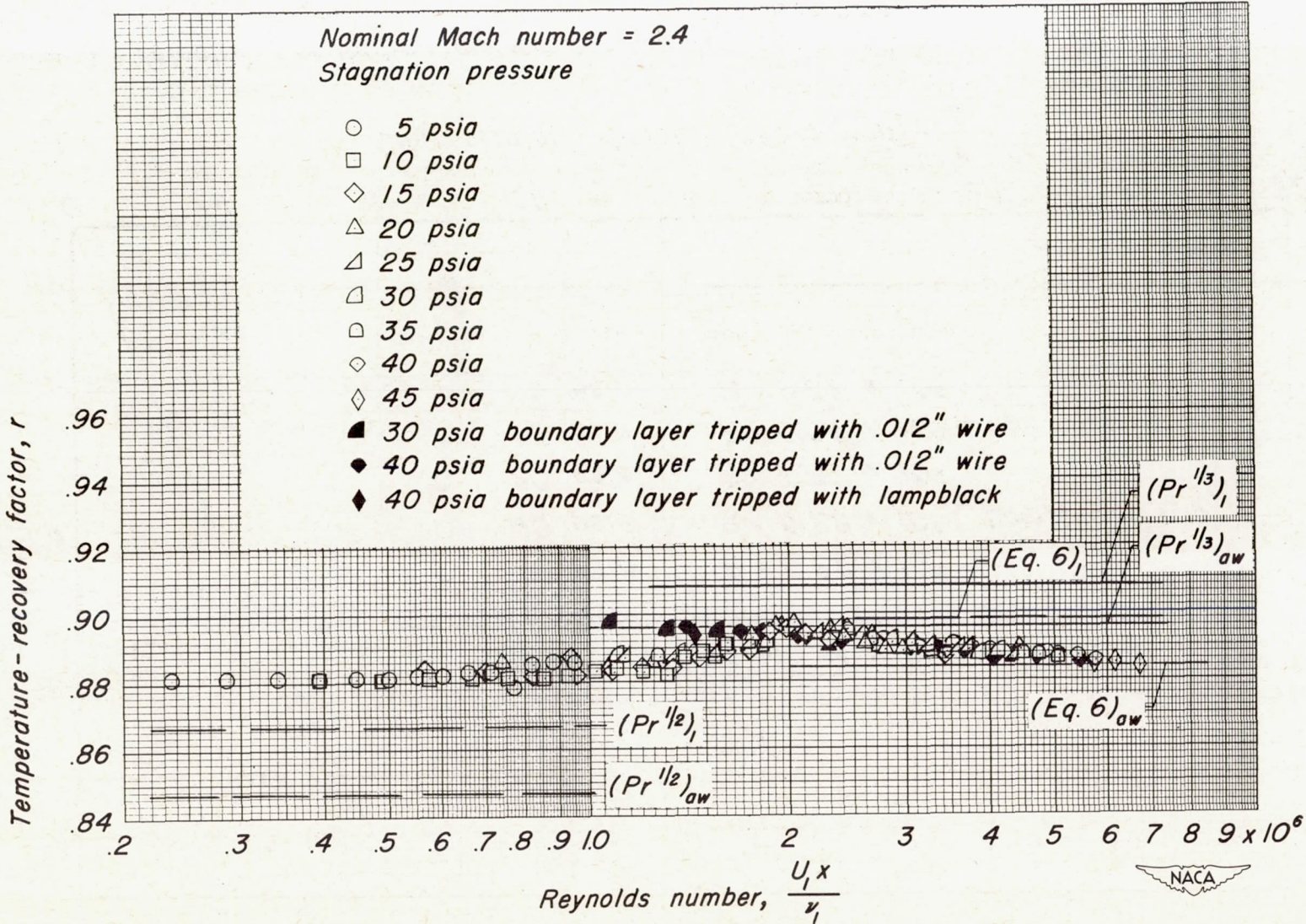


Figure 5.- Local temperature-recovery factor on flat plate.